Anal. Chem. **2002,** *74,* 5313−5320

RNA−Peptide Binding and the Effect of Inhibitor and RNA Mutation Studied by On-Line Acoustic Wave Sensor

Nardos Tassew* and Michael Thompson

Department of Chemistry, University of Toronto, 80 St. George Street, Toronto, ON, Canada M5S 3H6

Acoustic wave devices of the transverse shear-wave type are becoming increasingly important in the study of biochemical binding events at the solid−liquid interface in real time. The operation of the sensor is based on the principle that perturbations occurring at the solid−liquid interface result in changes in the propagating characteristics of the acoustic wave. The binding of the human immunodeficiency virus-type 1 Tat protein to the transactivation-responsive RNA element has been studied using this sensor. Variable acoustic signals in terms of frequency and motional resistance changes are obtained when surface-immobilized RNA is challenged by different peptide fragments derived from Tat protein. The effect of peptide concentration and mutation in addition to the inhibition of RNA−peptide binding by neomycin has been investigated. The results of this study suggest that acoustic physics offers considerable potential for the screening of small-molecule interactions with nucleic acids.

The human immunodeficiency virus type 1 (HIV-1) Tat protein belongs to the class of RNA-binding proteins that contain an arginine-rich basic motif that binds to the target RNA.[1] Proteins preferentially attach to secondary-structure elements of RNA, such as bulges and stem loops, through nucleic acid-binding domains of 60−90 amino acid sequences that mediate attachment.[2−4] The Tat protein is 86 amino acids long and regulates HIV gene expression by binding to the transactivation-responsive region (TAR) on mRNA transcripts, resulting in a stimulation of the efficiency of transcription. When Tat is absent, mRNA transcripts are terminated prematurely and replication of the virus is inhibited. In view of the important regulatory role that the protein plays in the life cycle of the virus, the TAR−Tat interaction constitutes a potential target for the development of antiviral drugs.[5−8] The HIV-1 TAR RNA has a conserved hairpin structure and spans nucleotides +1 to +59 of the viral mRNA. It has a duplex region interrupted by a trinucleotide bulge and a hexanucleotide loop (Figure 1). Chemical interference and mutational studies have shown that the regions necessary for Tat binding are the trinucleotide bulge (especially U23), base pairs G26, C39, and A27, U38, and the two phosphate groups located between the bulge and the lower stem.[9−11] The protein can be divided into two functionally different regions: the N-terminal activation domain (residues 1−48), which contains acidic, proline-rich, cysteine-rich and a core region; and the C-terminal RNA-binding domain (residues 49−72). The arginine-rich region (residues 49−59) in the RNA-binding domain is sufficient to bind to TAR; however, other amino acid residues outside this region contribute to the overall binding affinity and kinetic stability of the TAR−Tat complex.

It is common practice to use small peptide models in order to investigate complex RNA−protein binding interactions.[2] However, care must be taken to ensure that the smaller molecule reflects the behavior of the much larger protein moiety. Different studies have shown that short synthetic Tat peptides, which contain the argenine-rich basic region, bind to TAR RNA with an affinity and specificity similar to the full-length Tat protein[7,8] and thus are suitable to study TAR−Tat binding. Tat peptides, like most arginine-rich peptides, are unstructured in the unbound state.[12] This results in a structural adaptation to the unique shape and arrangement of electrostatic, hydrogen bond, and hydrophobic force distribution of TAR RNA.[3]

The specific mechanisms through which RNA recognition by proteins take place are poorly understood, and the structures of very few complexes have been solved by NMR spectroscopy and X-ray crystallography.[5,6,13,14] However, it is well established from various studies that binding usually takes place by an "induced fit" in which the protein, the RNA, or both, undergo conformational changes.[15] NMR studies have shown that TAR undergoes conformational changes and becomes more ordered when bound to

(1) Watson, K.; Edwards, R. J. *Biochem. Pharmacol.* **1999**, *58*, 1521−1528.
(2) *RNA-Protein Interactions*; Nagai, K., Mattay, I. W., Eds.; Frontiers in Molecular Biology Series; Oxford University Press: Oxford, U.K., 1994.
(3) Varani, G. *Acc. Chem. Res.* **1997**, *3*, 1189−195.
(4) Canadillas, J. M. P.; Varani, G. *Curr. Opin. Struct. Biol.* **2001**, *11*, 53−58.
(5) Jones, S.; Daley, D. T. A.; Luscombe, N. M.; Berman, H. M.; Thornton, J. M. *Nucleic Acids Res.* **2001**, *29*, 943−954.
(6) Farrow, M. A.; Aboul-ela, F.; Owen, D.; Karpeisky, A.; Beigleman, L.; Gait, M. J. *Biochemistry* **1998**, *37*, 3096−3108.
(7) Long, K. S.; Crothers, D. M. *Biochemistry* **1995**, *34*, 8885−8895.
(8) Mei, H. Y.; Mack, D. P.; Galan, A. A.; Halim, N. S.; Heldsinger, A.; Loo, J. A.; Moreland, D. W.; Sannes-Lowery, K. A.; Sharmean, L.; Truong, H. N.; Czarnik, A. W. *Bioorg. Med. Chem.* **1997**, *5*, 1173−1184.
(9) Hamy, F.; Asseline, U.; Grasby, J.; Iwai, S.; Pritchard, C.; Slim, G.; Butler, P. J. G.; Karn, J.; Gait, M. J. *J. Mol. Biol* **1993**, *230*, 111−123.
(10) Weeks, K.; Crothers, D. M. *Cell* **1991**, *66*, 577−588.
(11) Tao, J.; Frankel, A. D. *Proc. Natl. Acad. Sci. U.S.A.* **1992**, *89*, 2723−2726.
(12) Tan, R.; Brodsky, A.; Williamson, J. R.; Frankel, A. D. *Semin. Virol.* **1997**, *8*, 186−193.
(13) Hoffmann, S.; Willbold, D. *Biochem. Biophys. Res. Commun.* **1997**, *235*, 806−811.
(14) Tan, R.; Frankel, A. D. *Proc. Natl. Acad. Sci. U.S.A* **1995**, *92*, 5282−5586.
(15) Leulliot, N.; Varani, G. *Biochemistry* **2001**, *40*, 7949−7956.

10.1021/ac025924e CCC: $22.00
Published on Web 09/19/2002

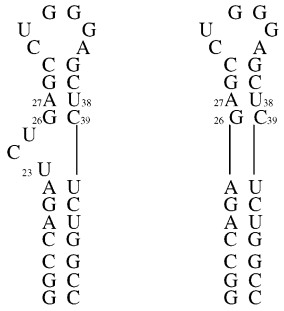

Figure 1. Secondary structure of HIV-1 TAR RNA and bulgeless TAR (MTAR), nucleotides G16−C46.

Tat. Generally, it possesses an A-form geometry with a bend of ∼50°, while the bulge region does not possess a very defined structure. The RNA adapts a more ordered conformation and becomes slightly distorted to the B-form with a bend of 10° on attachment of the protein.[12]

Most therapeutic small molecules are directed to affect protein chemistry,[16−18] and less has been accomplished in employing nucleic acids as targets for the design of new drugs. However, the latter approach constitutes an attractive strategy since RNA generation occurs first in the genetic expression pathway, and inhibition of its activity could prevent expression of many proteins.[18] Most therapeutic molecules targeted against RNA have been mainly aminoglycosides, such as neomycin, but other types of molecules continue to be screened to assess their suitability to be potential drugs.[18,19] The HIV-1 TAR−Tat interaction can be inhibited by aminoglycosides and amino acid and nucleotide analogues.[20−22] Disruption of TAR−Tat binding by small molecules is very useful for drug design since there is no cellular counterpart to TAR RNA and these molecules will be HIV specific, causing very little negative effect on other cellular functions.[23] Among the aminoglycoside antibiotics, neomycin has the greatest inhibitory effect on the binding of the Tat protein ($IC_{50} = 0.92$).[8] The positive charges on neomycin are attracted to the negatively charged RNA backbone, and its flexibility aids binding to RNA secondary structure by virtue of specific contacts.[19] It binds to the lower stem region of TAR as compared to Tat, which binds to the trinucleotide bulge and increases the dissociation constant of the protein.[20,22,24,25]

Techniques such as gel shift and filter binding assays have constituted the main approaches for the study of protein−nucleic acid interactions.[7,26] The application of biosensors to these binding studies, which is quite recent, possesses significant advantages over these traditional techniques, since radioisotope labels are not required and real-time data can be obtained from which important kinetic and affinity constants can be extracted. The thickness-shear mode (TSM) acoustic wave biosensor is based on the propagation of transverse waves in AT-cut piezoelectric quartz crystals. When these devices are employed in the liquid phase, the shear wave extends into the liquid beyond the crystal surface and decays exponentially. Thus, any perturbation in the propagation of the acoustic wave due to deposited mass, structural changes of surface species, slip, or interfacial coupling causes changes in acoustic parameters.[27−29] The response of the device is measured by acoustic network analysis, which generates multidimensional data (resonant frequency, phase angle, impedance, and equivalent circuit elements) for each frequency sweep. The TSM sensor employed in tandem with this method has been used in the study of DNA hybridization, blood platelet adhesion, and antibody−antigen interactions at interfaces.[30−32]

In the present paper, we report the application of the on-line TSM configuration to the study of RNA−protein and RNA−small molecule interaction at interfaces. A preliminary study of the binding of two Tat peptides (Tat-12 and Tat-40) to RNA was reported previously by Furtado et al.[32] In this study, the results in terms of the direction and shifts of the series resonant frequency were not consonant with the traditional mass-response model for the operation of the sensor in liquids. The present work is an extension of this study and involves examining the response for the interaction of TAR RNA with a larger number of peptides. The binding of Tat peptide fragments to TAR RNA and to a mutated version of TAR (MTAR), as well as the disruption of this binding by neomycin, has been examined in real time using acoustic wave propagation.

EXPERIMENTAL SECTION

Reagents and Materials. *TAR RNA Synthesis.* The, A, U, G, and C phosporamadites and the C-biotinTEG controlled-pore glass columns were purchased from Glen Research (Sterling, VA). Tetrazole/acetonitrile, 1-methyimidazole/THF, acetic anhydride/pyridine/THF, iodine/H_2O/pyridine, and anhydrous acetonitrile were obtained from Applied Biosystems (Mississauga, ON, Canada). Ammonium hydroxide, ethanol, TBAF, triethylamine, TEAA, TFA, acetonitrile, and sterile water were purchased from Sigma Aldrich (Oakville, ON, Canada).

Peptide Synthesis. The resins and amino acid residues were purchased from Advanced ChemTech (Louisville, KY). Dimethylformamide, *N*-methylpyrrolidone, piperidine, and HATU were obtained from Sigma Aldrich.

Radiolabeling. T4 polynucleotide kinase and T4 polynucleotide buffer were purchased form New England Biolabs. [γ-^{32}P]ATP

(16) Hermann, T.; Westhof, E. *J. Med. Chem.* **1999**, *42*, 1250−1261.
(17) Chen, Q.; Shafer, R. H.; Kuntz, I. D. *Biochemistry* **1997**, *36*, 11402−11407.
(18) Lind, K. E.; Du, Z.; Fujinaga, K.; Peterlin, B. M.; James, T. L. *Chem. Biol.* **2002**, *19*, 185−193.
(19) Schroeder, R.; Waldsich, C.; Wank, H. *EMBO J.* **2002**, *19*, 1−9.
(20) Mei, H. Y.; Cui, M.; Heldsinger, A.; Lemrow, S. M.; Loo, J. A.; Lowery, K. A. S.; Sharmeen, L.; Czarnik, A. W. *Biochemistry* **1998**, *37*, 14204−14212.
(21) Sullenger, B. A.; Gallardo, H. F.; Ungers, G. E.; Gilboa, E. *J. Virol.* **1991**, *65*, 6811−6816.
(22) Hamy, F.; Brondani, V.; Florsheimer, A.; Stark, W.; Blommers, M. J. J.; Klimkait, T. *Biochemistry* **1998**, *37*, 5086−5095.
(23) Gallego, J.; Varani, G. *Acc. Chem. Res.* **2001**, *34*, 836−843.
(24) Wang, S.; Wuber, P. W.; Cui, M.; Czarnik, A. W.; Mei, H. Y. *Biochemistry* **1998**, *37*, 5549−5557.
(25) Mei, H. Y.; Galan, A. A.; Halim, N. S.; Mack, D. P.; Moreland, D. W.; Sanders, K. B.; Truong, H. N.; Czarnik, A. W. *Bioorg. Med. Chem. Lett.* **1995**, *5*, 2755−2760.
(26) Churcher, M. J.; Lammont, C.; Hamy, F.; Dingwall, C.; Green, M. S.; Lowe, A. D.; Butler, P. J. G.; Gait, M. J.; Karn, J. *J. Mol. Biol.* **1993**, *230*, 90−110.
(27) Thompson, M.; Kipling, A. L.; Duncan-Hewitt, W. C. *Analyst* **1991**, *116*, 881−890.
(28) Cavic, B. A.; Hayward, G. L.; Thompson, M. *Analyst* **1999**, *124*, 1405−1420.
(29) Su, H.; Thompson, M. *Can. J. Chem.* **1996**, *74*, 344−358.
(30) Cavic, B. A.; Freedman, J.; Morel, Z.; Mody, M.; Rand, M. L.; Stone, D. C.; Thompson, M. *Analyst* **2001**, *126*, 342−348.
(31) Thompson, M.; Cavic, B. A.; Furtado, L. M.; Morel, Z.; Tassew, N. Acoustic Wave Study of Interfacial-Bound Proteins, Nucleic Acids and Blood platelets. In *Novel Approaches in Biosensors and Rapid Diagnostic Assays;* Liron, Z, Bromber, A., Fisher, M., Eds.; Kluwer Academic/Plenum Publishers: New York, 2000; pp 17−32.
(32) Furtado, L. M.; Su, H.; Thompson, M. *Anal. Chem.* **1999**, *71*, 1167−1175.

Tat-protein

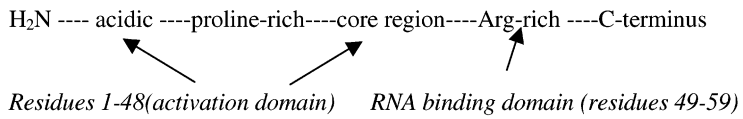

Tat peptides

Tat-12	H_2N-Tyr-Gly-Arg-Lys-Lys-Arg-Arg-Gln-Arg-Arg-Arg-Pro-OH
Tat-18	H_2N-Tyr-Gly-Arg-Lys-Lys-Arg-Arg-Gln-Arg-Arg-Arg-Pro-Pro-Gln-Gly-Ser-Gln-Thr-OH
Tat-20	H_2N-Tyr-Gly-Arg-Lys-Lys-Arg-Arg-Gln-Arg-Arg-Arg-Pro-Pro-Gln-Gly-Ser-Gln-Thr-His-Gln-OH
Tat-22	H_2N-Tyr-Gly-Arg-Lys-Lys-Arg-Arg-Gln-Arg-Arg-Arg-Pro-Pro-Gln-Gly-Ser-Gln-Thr-His-Gln-Val-Ser-OH
Tat-25	H_2N-Tyr-Gly-Arg-Lys-Lys-Arg-Arg-Gln-Arg-Arg-Arg-Pro-Pro-Gln-Gly-Ser-Gln-Thr-His-Gln-Val-Ser-Leu-Ser-Lys-OH
Tat-27	H_2N-Tyr-Gly-Arg-Lys-Lys-Arg-Arg-Gln-Arg-Arg-Arg-Pro-Pro-Gln-Gly-Ser-Gln-Thr-His-Gln-Val-Ser-Leu-Ser-Lys-Gln-Pro-OH
Tat-30	H_2N-Tyr-Gly-Arg-Lys-Lys-Arg-Arg-Gln-Arg-Arg-Arg-Pro-Pro-Gln-Gly-Ser-Gln-Thr-His-Gln-Val-Ser-Leu-Ser-Lys-Gln-Pro-Thr-Ser-Gln-OH

Figure 2. Schematic of HIV-1 Tat protein and the primary sequence of Tat peptide fragments containing the Arg-rich RNA-binding region.

was purchased from NEN Life Science Products (Boston, MA). Sterilized water, anhydrous ethanol, sodium ethanoate, chloroform, and EDTA were all purchased from Sigma Aldrich. Scinitillant vials were bought from Fisher Scientific (Nepean, ON, Canada).

Buffer. The buffers 1 M Tris HCl (pH 7.5), 5 M NaCl, and 0.5 M EDTA were all purchased from Sigma Aldrich.

Crystals. The 9-MHz AT-cut piezoelectric quartz crystals, coated with polished gold electrodes on both sides, were obtained from International Crystal Manufacturing (Oklahoma City, OK).

Instrumentation. *Flow Cell and Network Analyzer.* The TSM sensor's response in liquid was measured using an HP 4195 network/spectrum analyzer (Hewlett-Packard, Palo Alto, CA). The quartz crystal is placed between two halves of a Plexiglas flow cell with O-rings, in such a way that the electrodes are in electrical contact with the network analyzer. Only one face of the crystal is exposed to buffer and sample solutions, and the other face is kept dry by a continuously flowing nitrogen gas. The flow of nitrogen is extremely low (6 mL/min) such that it does not cause noise associated with turbulent flow. Buffer and sample solutions are introduced in a flow-through format using a peristaltic pump (four-channel EVA-pump model 1000). Data are taken every 30 s, and the values of the equivalent circuit element of the crystal are calculated internally by the analyzer from measured data. A PC is connected to the analyzer, and the frequency response is displayed on the screen in real time.

Procedure. *TAR RNA Synthesis and Characterization*. TAR RNA containing 31 bases (5′-GGC CAG AUC UGA GCC UGG GAG CUC UCU GGC C-3′) was chemically synthesized using 2′-*tert*-butyldimethylsilyl- and 5′-dimethoxytrityl-protected phosphoramadites on an Applied Biosystems 392 DNA/RNA synthesizer. Biotin was incorporated at the 3′ end during the synthesis. The oligoribonucleotide was desalted and detritylated using oligonucleotide purification cartridges (Poly Pak). The mass was confirmed by MALDI-MS. The RNA was dried and stored at −20 °C, and it was resuspended in Tris buffer (10 mM Tris, 70 mM NaCl, 0.2 mM EDTA) prior to use.

Tat Peptide Synthesis. All Tat peptides (Figure 2) were synthesized using standard Fmoc chemistry protocols. They were purified by reversed-phase HPLC using a linear gradient from water (0.1% TFA) to 70% acetonitile (0.1% TFA). The mass of the peptides was confirmed by electrospray mass spectrometry. The concentration was spectroscopically determined from tyrosine absorbance in 6 M guanidine hydrochloride (275.5 nm, $\epsilon = 1475$). [33]

RNA−Peptide Interaction and Acoustic Network Analysis. The interactions of various synthetic Tat peptide fragments with immobilized TAR RNA have been investigated. The peptides all contained the basic region required for binding, with the longer fragments containing more amino acid residues from the carboxy terminal. The crystals were cleaned with acetone, ethanol, and water and dried under a stream of nitrogen gas before use. All measurements were taken during a continuous flow, and the pump is only stopped momentarily in order to switch between solutions. Buffer was first flowed through the flow cell at a rate of 0.06 mL/min until a stable series resonant frequency was obtained. A 500-μL solution of neutravidin in Tris buffer (1 mg/ml) was then injected, followed by buffer to remove nonadsorbed protein from the surface. The frequency was left to stabilize, a 500-μL solution of 3′-biotinylated TAR RNA (1 μM in Tris buffer) flowed through, and the surface was washed with buffer until the frequency stabilized again at the new value. Then, 200 μL of analyte solution (Tat peptide, neomycin) was injected. The dependence of the frequency signal on concentration was investigated by injecting different concentrations of peptide solutions (1, 2.5, 5, 10, 25, 50, 100, and 200 μM). A set of control experiments was also performed at each concentration by injecting peptide on a neutravidin-modified surface in the absence of TAR RNA. For studies involving MTAR, the same procedures were followed as above, except a bulgeless TAR was immobilized on the surface. The binding of neomycin to TAR was investigated by flowing through various concentrations of the drug (1, 5, 10, 20, 50, and 100 μM) after

(33) Edelhoch, H. *Biochemistry* **1967**, *6*, 1948−1954.

TAR RNA was immobilized in the usual manner. A set of control experiments was performed to ascertain that the acoustic signals arise from specific binding of the drug to the RNA, by injecting neomycin after flowing through neutravidin. The disruption of TAR−Tat binding by neomycin was studied by injecting a solution of neomycin after Tat peptide was made to interact with TAR.

Quantification of Immobilized RNA. Radiochemical experiments were carried out in order to find out how much TAR RNA is immobilized on the surface. The experimental setup was the same as above, except no acoustic wave measurements were involved. The RNA was labeled with ^{32}P at the 5′ end. A mixture of the hot solution (20 μL, 35pmol) and that of cold TAR (480 μL, 465 pmol) in Tris buffer flowed though, following injection of neutravidin and the usual washoff with buffer. After TAR RNA was immobilized and the experiment was performed in the same manner as above, the crystal was taken out of the flow cell and put in 5 mL of scintillant and shaken well. The count for this solution was then measured (postexperiment count), it was compared with the count obtained for a solution taken before the experiment was carried out (pre-experiment count), and the amount of RNA immobilized was calculated.

RESULTS AND DISCUSSION

The immobilization of TAR RNA onto one electrode of TSM devices was effected using neutravidin−biotin chemistry. Neutravidin is a tetrameric protein and a deglycosylated derivative of avidin displaying similar binding affinity to biotin. However, it has a much reduced isoelectric point and exhibits less nonspecific binding than the parent molecule. [34] The protein is suitable for the immobilization of nucleic acids in a flow-through format since it adsorbs strongly to gold surfaces and forms a monolayer,[35] resulting in a significant frequency change. Neutravidin−biotin interaction is very strong and stable under most conditions ($K_d = 10^{-15}$); thus, the RNA remains attached to the surface during the course of the flow-through experiments. The immobilization of the nucleic acid on the crystal surface gives a frequency shift of ∼50 Hz, and the signal stays at the new value even after washing with buffer for prolonged periods of time, which indicates that the RNA is irreversibly immobilized on the surface. Studies have shown that only one of the four biotin-binding sites on neutravidin is available as a result of the surface interaction process. This is in agreement with results obtained from radiochemical labeling studies which indicate that ∼1 pmol of TAR is attached to the surface. Assuming close packing and taking into account the surface area occupied by the protein (∼100 nm^2) and the area available for immobilization (1.0 cm^2), ∼1 pmol would be found at the surface, yielding a 1:1 neutravidin−biotin stoichiometry.

Previous studies have shown that peptide fragments derived from Tat protein bind to TAR RNA with an affinity similar to that of the full-length protein in a 1:1 stoichiometry. [22,26,36] When a series of peptides (Tat-12, Tat-18, Tat-20, Tat-22, Tat-25, Tat-27, Tat-30) are allowed to interact with immobilized nucleic acid, variable changes in frequency and motional resistance signals are obtained (Table 1). The largest frequency shift is obtained for Tat-12, and the magnitude decreases as the peptide chain becomes longer (Figure 3). The binding of Tat-27 results in an almost zero frequency response whereas the direction of the signal reverses for Tat-30 (Figure 4). Previous work has shown that Tat-40 behaves in a manner similar to Tat-30, which appears to be the case for peptides longer than Tat-27. When the frequency shift for the binding of each peptide is plotted against the number of carbons in the peptide, a linear curve is obtained indicating that the sensor responds to these peptides in a quite predictable manner ($R^2 = 0.98$) (Figure 5). Initially, it appears that added mass from the peptides accounts for the signals that are obtained for the interaction of these peptides with the RNA. However, the magnitude and direction of the changes are completely different from the behavior predicted by the well-known Sauerbrey model,[37] confirming that mass is not the determining factor and that other interfacial conditions clearly govern the signals. The smaller peptides (Tat-12−Tat-25) result in frequency increases, which is the precise reverse of the result predicted by the mass-response model. Moreover, the difference in magnitude of frequency obtained for the peptides cannot be accounted by the difference

Table 1. Frequency Changes for the Binding of Peptides on a TSM Sensor as Compared to Values Predicated by the Mass-Response Model

compd	formula wt (g/mol)	ΔF predicted by Saurebrey's eq (Hz)[a]	max ΔF for binding to TAR (Hz)[b]
Tat-12	1658.98	−0.30	33 ± 2
Tat-18	2255.59	−0.41	26 ± 1
Tat-20	2520.85	−0.46	20 ± 1
Tat-22	2707.06	−0.50	15 ± 1
Tat-27	3260.72	−0.60	0.5 ± 1
Tat-30	3577.03	−0.65	−34 ± 2

[a] Values are calculated by assuming 1 pmol of Tat on the surface (based on the amount of RNA immobilized from radiochemical measurements and a stoichiometry of 1:1 TAR−Tat binding). [b] Values are the average of three different determinations.

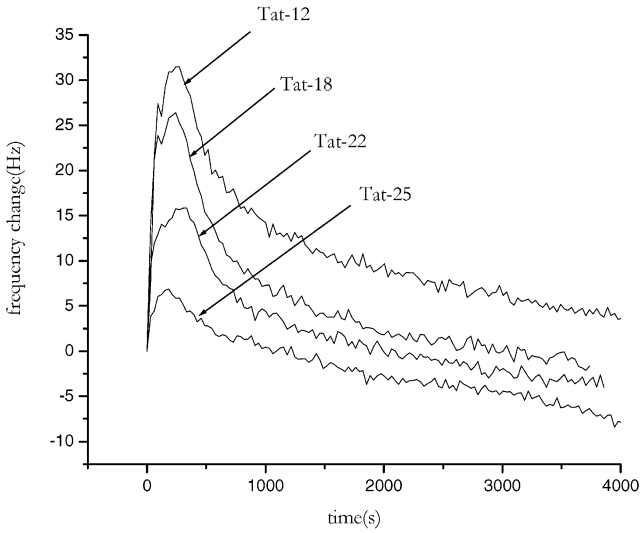

Figure 3. Changes in series resonant frequency for the binding of Tat peptides to immobilized TAR RNA.

(34) Hiller, Y.; Gershoni, J. M.; Bayer, E. A.; Wilchek, M. *Biochem. J.* **1987**, *248*, 167−171.
(35) Ebersole, R. C.; Miller, J. A.; Moran, J. R.; Ward, M. D. *J. Am. Chem. Soc.* **1990**, *112*, 3239.
(36) Summer-Smith, M.; Roy, S.; Barnett, R.; Reid, L. S.; Kuperman, R.; Delling, U.; Sonenberg, N. *J. Virol.* **1991**, *65*, 5196−5202.
(37) Sauerbrey, G. *Z. Phys.* **1959**, *155*, 206.

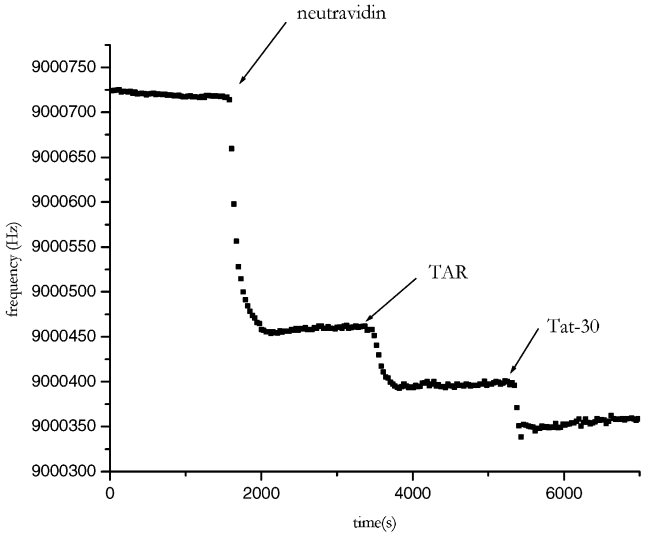

Figure 4. On-line frequency response for the interaction of Tat-30 with TAR RNA.

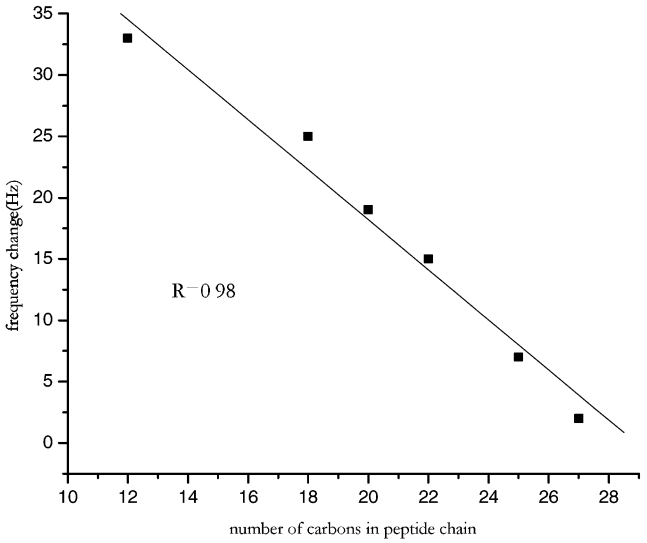

Figure 5. Linearity of frequency response to the number of carbons in peptide chain (Tat-12−Tat-27).

in added mass in proceeding from a smaller to a larger peptide. For example, there is a mass difference of 596.6 g/mol between Tat-12 and Tat-18, which would translate to a frequency difference of 0.1 Hz according to the mass-response model. However, a frequency difference of 7 Hz is obtained in the present study. Accordingly, we conclude that the frequency signal results from a competitive combination of various interfacial parameters, rather than absolute mass. The results from Tat-27 are specially revealing in that various competing factors are clearly at play in determining the acoustic signals, since the frequency change is almost zero even though there is added mass on the device surface.

One important factor contributing to the frequency signal may be the structural changes instigated in the nucleic acid as a result of the binding of peptide. The bases at the bulge become stacked and the RNA stiffens in the bound state giving rise to rigid and flexible regions.[15] This causes the various layers to move at different velocities yielding, in turn, changes in acoustic coupling and energy dissipation, which results in frequency and motional resistance changes. Another factor affecting the signal may be

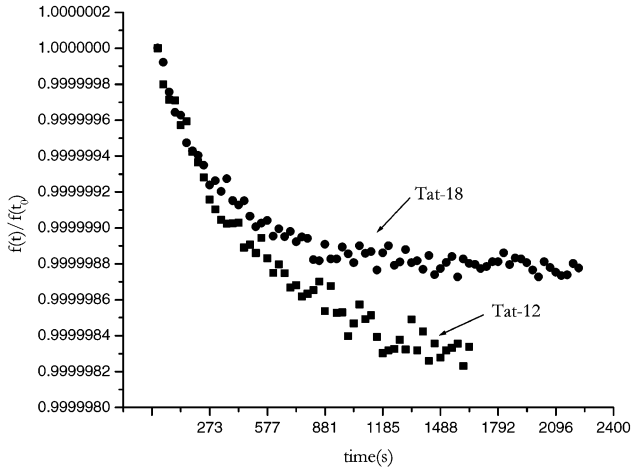

Figure 6. Comparison of the dissociation kinetics of the Tat-12−TAR and Tat-18−TAR complex. Data for the Tat-12−RNA complex are indicated by squares and for the Tat-18−RNA complex by circles.

the change in the free energy of the surface following peptide binding, with the larger peptides being expected to "cover" a greater area on the nucleic acid. Such an effect is known to perturb coupling between the surface and liquid which, in turn, leads to changes in acoustic parameters. In summary, various factors affect the propagation of the acoustic wave at the interface (structural changes, slip, coupling), and the isolation of the individual contribution of each of these to the frequency signal represents a significant problem in acoustic physics. This renders the biophysical interpretation of data from TSM studies very difficult to contemplate. On the other hand, unlike, for example, surface plasmon resonance detection, acoustic physics offers a unique opportunity to provide useful information on the chemistry of bimolecular binding such as structural changes and other interfacial phenomena.

The binding of the peptides to TAR RNA is reversible, as shown by the recovery of the frequency signal to the baseline when the device is washed with buffer. Thus, the stability of the different peptide−RNA complexes can be studied by direct examination of the decay of the response curve. Unlike the smaller peptides, the binding of Tat-30 results in a frequency decrease with the signal taking much longer to return to the baseline level, showing that this peptide forms a significantly more stable complex. This is reasonable in view of the additional intermolecular interactions associated with the inclusion of more amino acid residues from the C-terminus. Similar results are also obtained for the decay curve of Tat-18 and Tat-12 as shown in Figure 6, where it can be seen that the TAR−Tat-18 complex is also subject to a reduced dissociation rate. In their study of the binding of Tat peptide fragments to TAR RNA by gel shift assay, Long and Crothers[7] also observed similar behavior among various peptides, showing, importantly, that the same mechanism is involved for surface-bound interactions as is evident in the solution phase.

A set of control experiments was performed to ensure that the response of the sensor arises from genuine binding events and does not originate from nonspecific adsorption. The frequency response was almost zero on introduction of the peptides to the neutravidin-modified surface, although a small shift in motional resistance was observed (Figure 7). The two parameters are

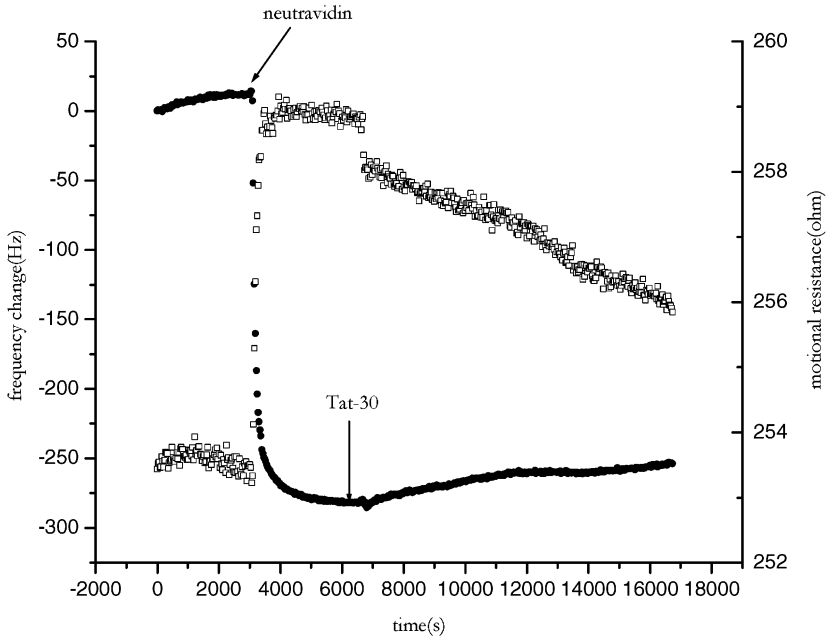

Figure 7. Control experiment involving the introduction of Tat-30 on a neutravidin-modified surface. Frequency data are indicated by closed circles and motional resistance by open squares.

governed by different factors, and accordingly, analysis of both provides additional information concerning the particular biomolecular interaction under study. Previous experiments involving ^{125}I-labeled peptide indicate that significant nonspecific adsorption of peptide occurs on the neutravidin surface,[32] although no corresponding frequency shift is found. This result is not surprising given the relatively small size of the peptides (<4 kDa), compared to the much larger neutravidin molecule (65 kDa), which will, therefore, not result in a significant change of interfacial properties. However, the binding of biotinylated TAR, which is not much larger than the peptides, to neutravidin, causes a frequency response of 50 Hz, showing that a specific bimolecular interaction can instigate changes in surface properties that are detectable by the sensor. This again confirms that mass is not a significant factor in determining the response.

For studies involving different concentrations of peptides, an increase in response is observed when the concentration is increased, leveling off subsequently as surface saturation is achieved (Figure 8). The plot of frequency change versus concentration of the peptide is made by assuming that the surface concentration is proportional to solution concentration. The experiments were performed at a high enough flow rate (60 μL/min) such that binding is unlikely to be diffusion limited. Flow rates of up to 4 times the above value were employed and no appreciable differences in binding were found, indicating that the reaction is not under diffusion control. Thus, useful data concerning binding kinetics can be obtained through analysis of the association curve. Maximum frequency changes following binding were observed when saturation level concentrations were employed, which is in the range of 70 μM for most of the peptides. Using this concentration ensures the maximum amount of bound RNA on the surface leading to maximum frequency changes. However, if concentrations are further increased beyond what is required for saturation, the signal begins to decrease. This is likely

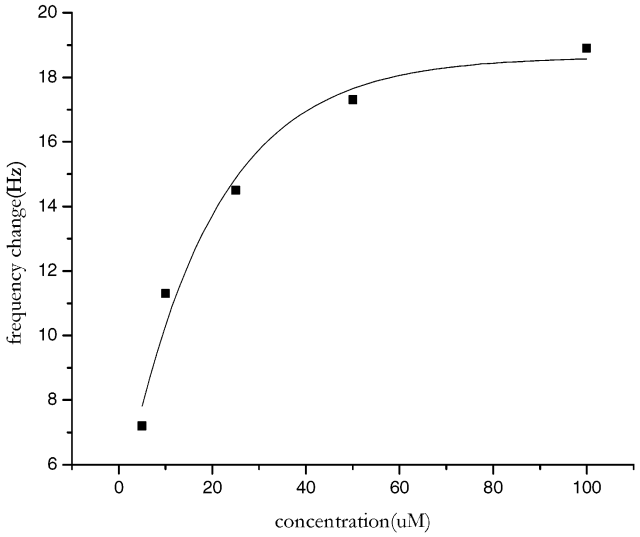

Figure 8. Frequency−concentration plot for the binding of Tat-20 to TAR RNA (5, 10, 25, 50, and 100 μM).

caused by the formation of secondary and ternary RNA−peptide complexes at very high concentrations, as suggested by other studies.[38]

It is suggested in the literature that there is a 7−10-fold decrease in transactivation levels when mutation is introduced to the bulge region of TAR.[7,10,11] When mutated TAR (which lacks the trinucleotide bulge, MTAR) is allowed to interact with the peptides, smaller frequency changes are obtained compared to the parent RNA, indicating that the bulge is required for Tat binding (Figure 9). Binding to MTAR is expected in view of the fact that many RNA-binding proteins attach weakly to such nucleic acid moieties regardless of sequence or structure. However, the

(38) Sannes-Lowery, K. A.; Hu, P.; Mack, D. P.; Mei, H. Y.; Loo, J. A. *Anal. Chem.* **1997**, *69*, 5130−5135.

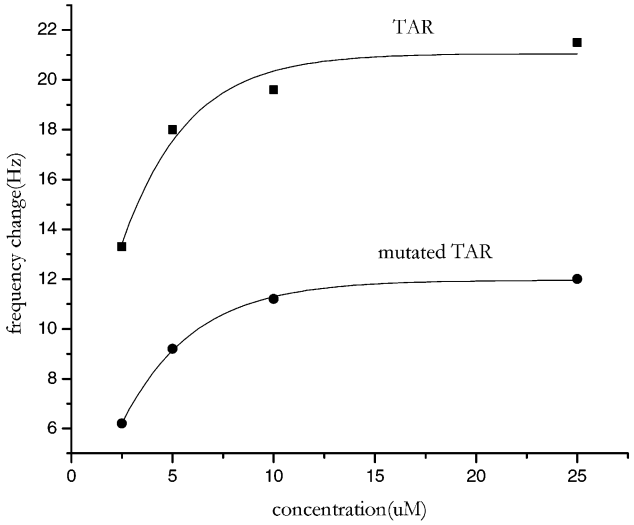

Figure 9. Frequency−concentration plot showing reduced binding of Tat-20 to MTAR compared to wild-type TAR. Concentrations of peptide are 2, 5, 10, and 25 μM. Data for the binding of the peptide to TAR are indicated by squares and for MTAR by circles.

Table 2. Comparison of Frequency Changes for the Binding of Peptides to TAR and MTAR

	ΔF (Hz)	
peptide	when binding to TAR	when binding to MTAR
Tat-12	33	23
Tat-18	26	12
Tat-20	20	11

discriminating ability of the Tat peptides has been found to increase when more amino acid residues are incorporated into the RNA-binding basic region.[7] Our results confirm this fact since the difference in the frequency value obtained for interaction with wild-type TAR, as opposed to mutated TAR, is greatest for the longer Tat peptides (Table 2). Biological function requires that proteins discriminate relevant RNA targets in the presence of all other noncognate RNAs in living cells. The ability to discriminate is due to the difference in binding energy, which arises from a unique arrangement of intermolecular forces, as well as the ability of the RNA to fold around the protein together with the energetic penalties associated with this process.[3,15,16,39] The binding specificity of Tat peptides shows an excellent correlation with the in vivo activity of the protein, as suggested in the literature.[2,40,41]

An increase in frequency is obtained for the binding of neomycin to TAR at different concentrations as shown in Figure 10a. Neomycin binds to the TAR and TAR−Tat complex but not to the Tat peptide.[8] Also, it does not attach to the underlying neutravidin layer as evidenced by control experiments (not shown). The plot of neomycin concentration versus maximum frequency change shows saturation around 100 μM (Figure 10b). When a solution of neomycin interacts with a preformed TAR−Tat complex on the device surface (Figure 11), a positive frequency shift is obtained indicating that a ternary complex of

(39) Draper, D. E. *J. Mol. Biol.* **1999**, *293*, 255−270.
(40) Weeks, K. M.; Crothers, D. M. *Biochemistry* **1992**, *31*, 10281−10287.
(41) Calnan, B. J.; Biancalana, S.; Hudson, D.; Frankel, A. D. *Genes Dev.* **1991**, *5*, 201−210.

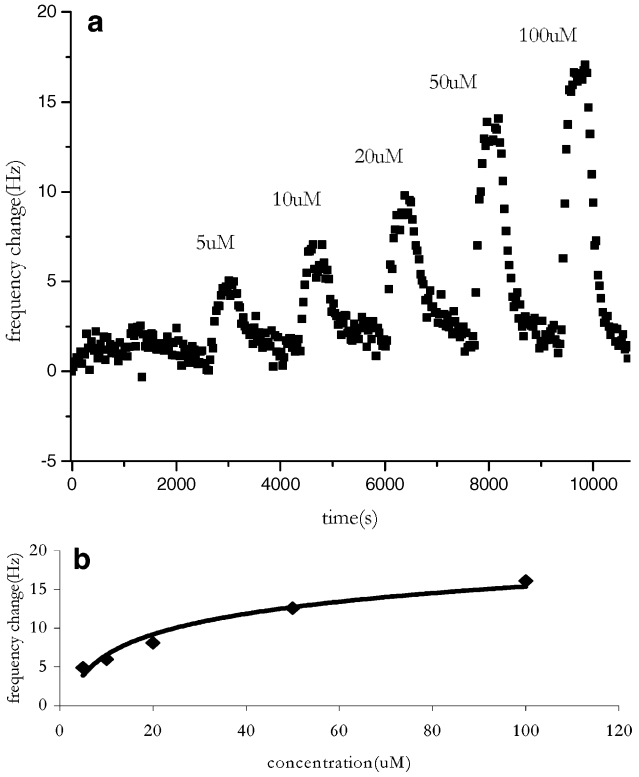

Figure 10. Frequency−time (A) and frequency−concentration (B) plots for the reversible binding of neomycin to TAR RNA.

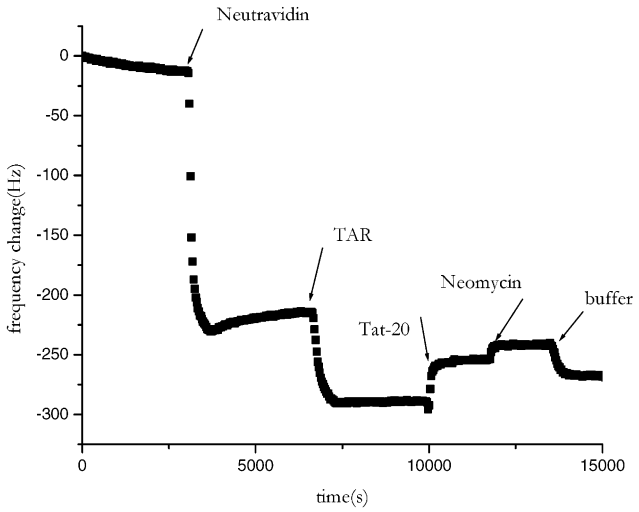

Figure 11. Response plot for the formation of a ternary TAR−peptide−neomycin complex.

TAR−Tat−neomycin is formed, as suggested by other studies.[22,24] On the other hand, when the Tat peptide binds to the TAR−neomycin complex, there is no significant frequency shift indicating that the formation of the TAR−Tat complex is inhibited. As shown in Figure 12, when Tat first binds to the TAR−neomycin complex, a momentary dip occurs in the frequency response, but the signal returns to the baseline without washing with buffer. This result is in agreement with other studies which showed that neomycin changes the RNA conformation to one unsuitable for peptide binding facilitating the dissociation of the Tat peptide from TAR RNA.[24,42] Neomycin inhibits the TAR−Tat interaction in the range of 0.1−1 mM.[24,43] The lowest concentration of this range

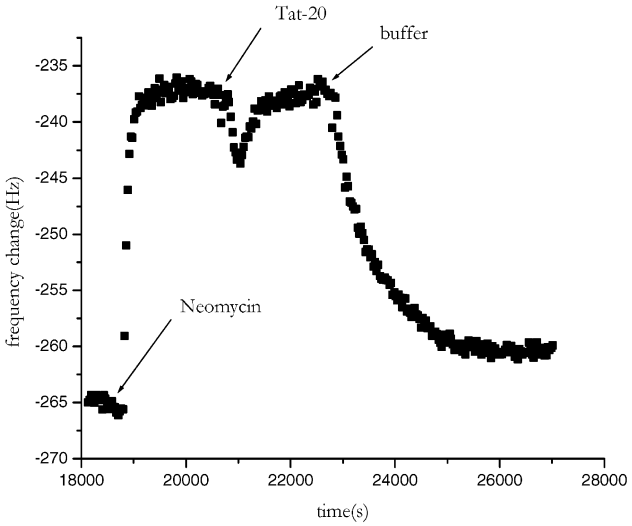

Figure 12. Frequency−time plot for the inhibition of Tat-20 binding to preformed the TAR−neomycin complex on the sensor surface.

was used in the present study and was found to be effective in disrupting TAR−Tat binding. Additional experiments are underway to test other TAR−Tat inhibitors and compare their effectiveness. We believe that the TSM sensor is a particularly sensitive technique for the examination of the inhibitory effect of neomycin on TAR−Tat binding, and accordingly, this protocol can be extended to the screening of other small molecules that inhibit nucleic acid−protein binding.

CONCLUSIONS

A number of techniques are available for the study of solution-phase RNA−protein and RNA−small molecule binding, where other than simple "yes−no" information is required. Among these, NMR spectroscopy and mutagenesis experiments provide detailed structural information, but are obviously not suitable for on-line screening. Gel shift and filter binding assays provide binding constants for biomolecular interactions, but these methods are time-consuming and involve the use of radioisotope and fluorescence tags in the analysis. On-line study of protein−nucleic acid binding can be effected in a facile manner by both the surface plasmon resonance technique and acoustic physics, since neither method involves the use of such labels. The former approach measures the additional optical mass as a singularly change in resonance units, that is, no interfacial information is implied aside from what can be gleaned form thickness considerations. Transverse wave acoustic physics is clearly competitive from a sensitivity standpoint, but additionally, the method offers a number of parameters that can be utilized to examine nucleic acid−ligand interfacial chemistry. Such a possibility represents an advance in the chemical information that can be provided in low-to-medium throughput screening technology. However, future research efforts on model systems will be mandatory in order to dissect the links between interfacial structure and acoustic network parameters.

(42) Faber, C.; Sticht, H.; Schweimer, K.; Rosch, P. *J. Biol. Chem.* **2000**, *275*, 20660−20666.
(43) Litovchick, A.; Evdokimov, A. G.; Lapidot, A. *FEBS Lett.* **1999**, *445*, 73−79.

ACKNOWLEDGMENT

The authors are very grateful to the Natural Sciences and Engineering Council of Canada for support of this work. They also thank A. G. Woolley for allowing the use of facilities for peptide synthesis and G. Hayward of the University of Guelph for much helpful discussion.

Received for review July 8, 2002. Accepted August 19, 2002.

AC025924E